

This Page Is Inserted by IFW Operations
and is not a part of the Official Record

BEST AVAILABLE IMAGES

Defective images within this document are accurate representations of the original documents submitted by the applicant.

Defects in the images may include (but are not limited to):

- BLACK BORDERS
- TEXT CUT OFF AT TOP, BOTTOM OR SIDES
- FADED TEXT
- ILLEGIBLE TEXT
- SKEWED/SLANTED IMAGES
- COLORED PHOTOS
- BLACK OR VERY BLACK AND WHITE DARK PHOTOS
- GRAY SCALE DOCUMENTS

IMAGES ARE BEST AVAILABLE COPY.

**As rescanning documents *will not* correct images,
please do not report the images to the
Image Problem Mailbox.**

AN EXPLANATION FOR THE CONTROLLED RELEASE OF MACROMOLECULES FROM POLYMERS

Rajan Bawa*, Ronald A. Siegel**, Brian Marasca, Marcus Karel and Robert Langer***

Departments of Applied Biological Sciences, Chemical Engineering, Electrical Engineering and Computer Science, and The Whitaker College of Health Sciences, Technology, and Management, Massachusetts Institute of Technology, Cambridge, MA 02139 (U.S.A.)

and

Department of Surgery, Boston Children's Hospital, Boston, MA 02115 (U.S.A.)

(Received September 4, 1984; accepted in revised form January 3, 1985)

Controlled release systems composed of hydrophobic polymers such as ethylene-vinyl acetate copolymer have proven useful for releasing various polypeptides and other macromolecules for over 100 days. However, the release mechanism has never been elucidated. Evidence by microscopy is presented suggesting that release occurs through interconnecting pores formed by the macromolecules themselves. A mathematical model has been developed and used to predict the release rates of different proteins.

INTRODUCTION

Biocompatible polymers, such as ethylene-vinyl acetate copolymer (EVAc), permit the controlled release of macromolecules [1]. These polymer systems have a wide variety of applications. For example, EVAc polymers have been used as release systems for chemotactic [2,3] and growth factors [4,5], as components of bioassays for informational macromolecules [6,7] and histochemical markers in neurological studies [8,9], and also as delivery systems for insulin [10], interferon [11], and antigens [12]. However, the mechanism by which macromolec-

ular release occurs has not been elucidated. The polymers used are impermeable to molecules larger than 600 daltons; nonetheless, complete release of substances as large as 2×10^6 daltons for over 100 days has been demonstrated [1]. We now report that the incorporation of macromolecules into the normally non-porous polymer matrix results in formation of a tortuous, interconnected pore network. It is suggested that diffusion of the macromolecules through this network provides the basis for controlled release.

MATERIALS AND METHODS

Kinetic studies

Bovine serum albumin (BSA) ($M_w = 69000$), β -lactoglobulin A ($M_w = 37000$), and lysozyme

*Present address: Bausch and Lomb Inc., Rochester, NY, U.S.A.

**Present address: School of Pharmacy, University of California, San Francisco, CA 94143, U.S.A.

***To whom correspondence should be addressed at MIT.

APRIL 1985

bles.
-127

..... 169

..... 177

..... 183

se

..... 191

..... 197

..... 205

..... 217

..... 225

..... 233

..... 239

..... 247

..... 249

duced rates are

, India, Israel,

r copies by a

t.

Netherlands.

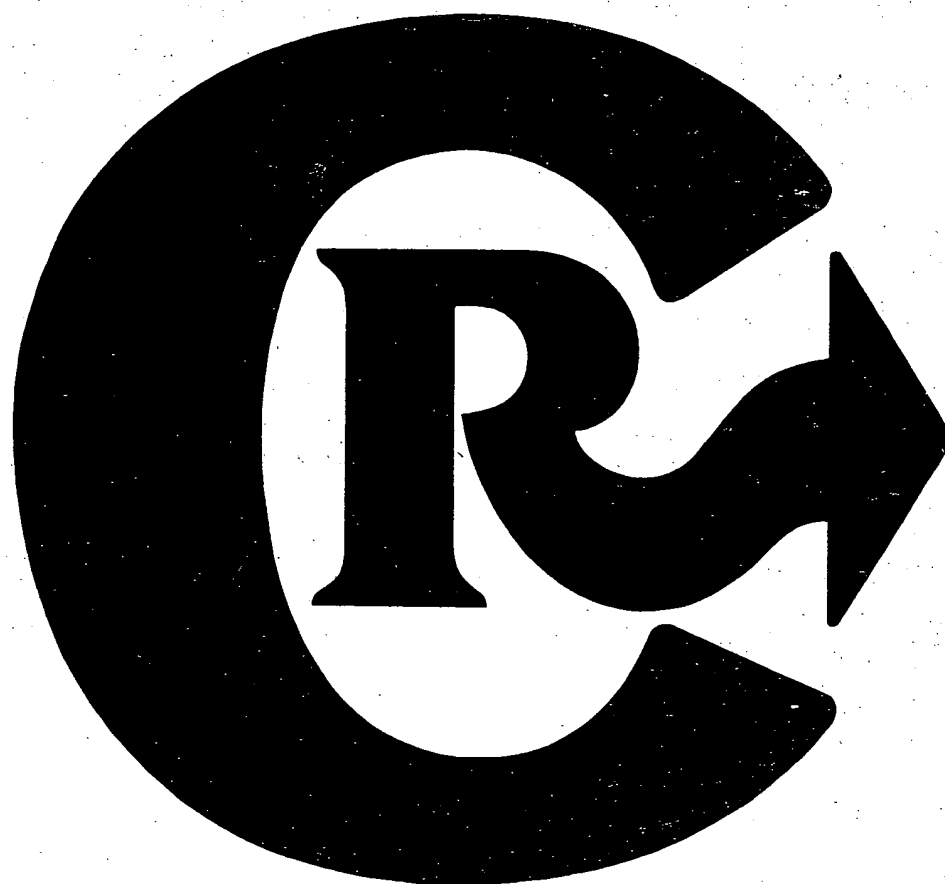
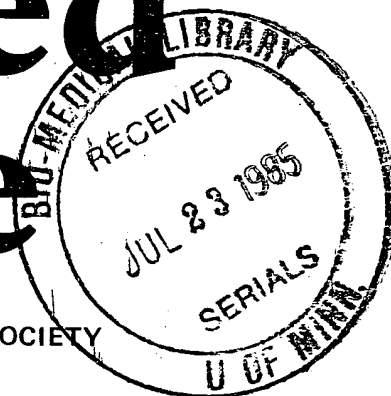
t be honoured

sevier Science

(2) 916-1250.

journal of controlled release

OFFICIAL JOURNAL OF THE CONTROLLED RELEASE SOCIETY



Elsevier

($M_w = 14000$) (all from Sigma Chemical Co., St. Louis, MO) powders were sieved into specified particle size ranges [13]. Each protein powder was dispersed in a 10% (w/v) ethylene-vinyl acetate (Elvax 40P, DuPont, 40% by weight vinyl acetate, washed with solvents to remove impurities [14]) solution in methylene chloride, and the suspensions were cast in a flat glass mold at -80°C . The low temperature caused the mixtures to congeal quickly, preventing drug migration. The resulting sheets were dried in two 48-hour stages, first at -20°C , and then under vacuum at 20°C [13].

To test release kinetics, nine $1\text{ cm} \times 1\text{ cm} \times 1\text{ mm}$ slabs were cut from each sheet, and coated on five faces using paraffin [13], leaving one $1\text{ cm} \times 1\text{ cm}$ face exposed. Two straightened stainless steel autoclips were then pressed into the paraffin on the back of each slab to anchor it down when placed in the release medium. The release medium (0.9% NaCl solution) was placed in 10 ml amounts into 20 ml scintillation vials. The slabs were placed on a shaker as described previously [15]. At each time point, slabs were moved to vials containing fresh saline, and the old solutions were spectrophotometrically (280 or 220 nm) assayed for protein content [13].

Protein particle densities were determined using a pycnometer with methylene chloride as the solvent. Before release, the porosity of a slab was determined by dividing the protein concentration in the slab by the protein particle density. At the end of the release experiment, porosity was again assessed by liquid leaching of salicylate [15]. In general, the porosity values before and after release agreed to within 5%. Thickness of the polymer slabs was measured using a micrometer (Stamet Co., Athol, MA). The standard deviation for thickness measurements ($n = 8$) was less than 4% for each slab.

Microscopic studies

For optical microscopy, the following procedure was used: $10\text{ }\mu\text{m}$ thin sections

were obtained using a cryogenic microtome set at -25°C , together with a microtome knife (Cryo-Cut Cryostat Microtome, Model 845 with a $4\frac{3}{4}$ " microtome knife Type 942, American Optical Corp., Scientific Instruments Division, Buffalo, NY). One milliliter of embedding medium (Tissue-Tek II O.C.T. Compound 4583, Lab-Tek Products Division, Miles Inc., Naperville, IL) was poured onto the chucks. After 30 seconds, it froze into an opaque solid, which was then planed by cutting thin sections off its top surface. Next, about $3\text{ mm} \times 1\text{ mm} \times 1\text{ mm}$ of release matrix was excised from various locations in the original $1\text{ cm} \times 1\text{ cm} \times 1\text{ mm}$ slab. This piece of matrix was then placed on the planed embedding medium such that one of the $3\text{ mm} \times 1\text{ mm}$ faces corresponding to a cross-section of the matrix was in contact with the planed surface. The matrix so oriented was then buttressed by more embedding medium which also hardened after 20 seconds in the machine.

Sections of $10\text{ }\mu\text{m}$ in thickness were then cut, and stuck of their own accord to the knife. These were retrieved by contact with a glass slide at room temperature. The final sections thus obtained were $3\text{ mm} \times 1\text{ mm} \times 10\text{ }\mu\text{m}$, the 1 mm representing the original depth of the matrix.

For observation under scanning electron microscopy (SEM), the following procedure was followed: The slabs, having been exposed to the release medium (0.9% saline), were dried in order to enable the high vacuum conditions necessary for SEM. To prevent deformation during drying of the pliable wet slab matrices, a critical point drying machine (Model 11-120A, Balzers Union, Liechtenstein) was used. The wet slab was placed in the chamber of the machine and the water in the sample replaced by 100% ethanol. The ethanol was then replaced by 100% amyl acetate, which is miscible with liquid carbon dioxide. The chamber was then cooled to 4°C and filled with liquid carbon dioxide. Carbon dioxide vapor was slowly exhausted to air while refilling the chamber with more carbon dioxide liquid to remove

the
dryin
and
soon
achie
liqui
occu
press
creas
samp
Coat
Corp
with
samp
whic

Drug

Sl
relea
At
and

Fig.
copo
Parti
after

the amyl acetate from the sample. The drying chamber was then heated to 40°C and the pressure increased to 85 atm. As soon as this temperature and pressure were achieved (15–20 min), the change from liquid to vapor phase of carbon dioxide occurred, and the sample was dry. The pressure and temperature were then decreased to ambient conditions*. The dried samples were then coated using an Economy Coater Type CVE-15 (Consolidated Vacuum Corporation, Rochester, NY) under vacuum with carbon and gold. The dried and coated samples were stored in tightly capped vials which were placed in a desiccator.

Drug distribution studies

Slabs containing BSA (50% loading) were released into 100 ml volumes of 0.9% NaCl. At various timepoints, a slab was removed and frozen on dry ice to terminate release.

A cryomicrotome (Damon/IEC, -25°C) was used to serially cut 10 μ m sections from the partially released polymer matrices. Four samples, representing four consecutive 10 μ m sections, were then released into 10 ml 0.9% NaCl solution for three days. The release medium was then filtered to remove wax, polymer, and embedding medium. Protein concentration was determined by UV spectroscopy at 220 nm [13].

RESULTS AND DISCUSSION

Viewed under an optical microscope, EVAc films cast without proteins appear as non-porous sheets (Fig. 1a). Slabs cast with proteins and sectioned prior to release

*Alternative procedures for preparing EVAc slabs for SEM have been developed recently [16].

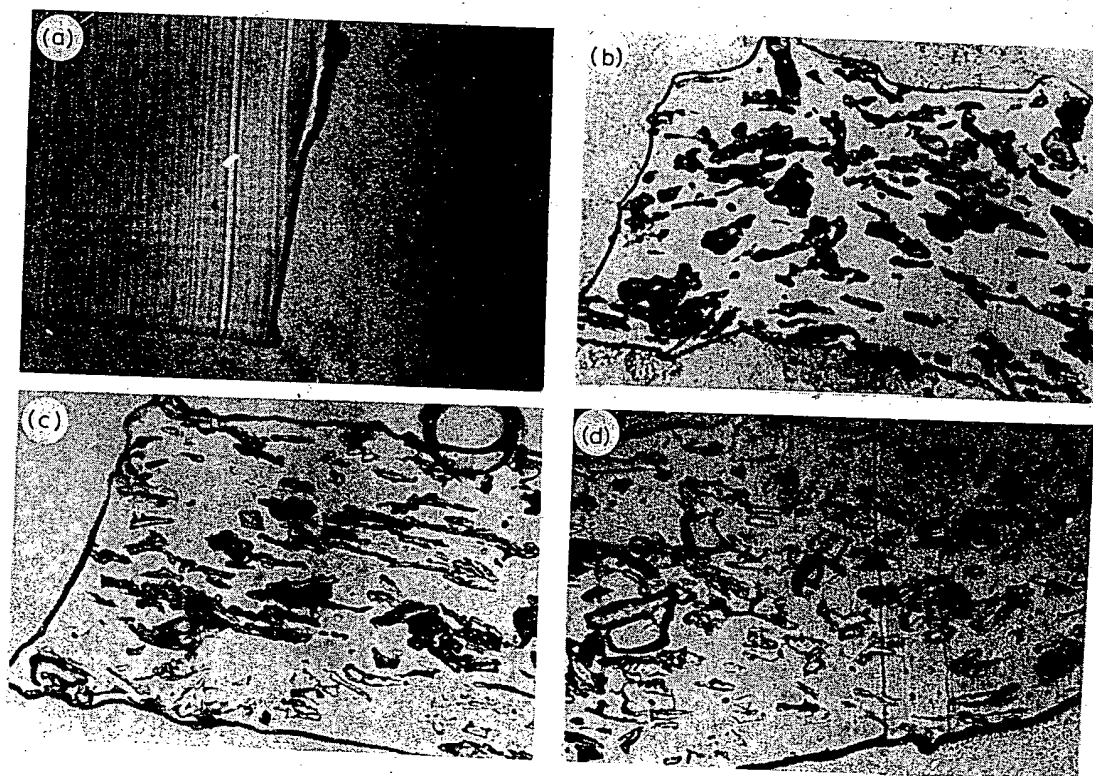


Fig. 1. Optical microscopy (OM) micrographs of controlled release polymers: (a) pure ethylene-vinyl acetate copolymer cast without drug (lines represent knife marks); (b) 25% by weight bovine serum albumin (BSA, particle size 63–149 μ m) matrix, prior to release; (c) slab similar to (b) after 16 h release; (d) slab similar to (b) after 40 h release. Slabs released to exhaustion have same appearance as (d) [25].

display areas of either polymer or protein (Fig. 1b). Slabs initially cast with proteins and released to exhaustion (5 months) appear as porous films (Fig. 1d). Pores with diameters as large as 100 μm , the size of the sieved particles, were observed. The structures visualized were also confirmed by Nomarski (differential interference contrast) microscopy. It appears that although pure EVAc is impermeable to macromolecules [1], molecules incorporated in the matrix dissolve once water penetrates the matrix and are then able to diffuse to the surface through pores created as the particles dissolve.

The scanning electron micrographs in Fig. 2 show that the pores are interconnected through narrow passageways. The passageways are necessary to permit movement of the macromolecules between pores.

Changes in pore structure over time were investigated. Sections were prepared from matrices in the process of release (Figs. 1b–d). We observed that (1) the pore structure changes minimally as a function of time, (2) after 16 or 40 hours there is no evidence of a receding interface between dissolved and

dispersed drug (Figs. 1c,d), and (3) none of the drug remains undissolved at 40 h (30% release). Observations (2) and (3) differ from those reported for less soluble low molecular weight drugs such as certain steroids [17], and are probably due to the high solubilities of many proteins such as BSA (solubility > 500 mg/ml) [18].

Figure 3 shows kinetic curves for BSA slabs of various drug particle sizes and loadings. The captions indicate the corresponding measured porosities.

We have made a number of assumptions in the development of a model: (1) The rate-limiting step for transport is drug diffusion through pores (other steps such as water penetration into the pores and drug dissolution occur in less than 40 h (Figs. 1c, d)). (2) The effect of concentration dependence on the drug diffusion coefficient is not significant [19]. (3) No drug diffusion occurs through the polymer backbone [1]. (4) The pores are interconnected (Figs. 1b–d, 2a,b), the porosity is uniform, and pore size changes minimally with time (Figs. 1b–d). (5) The initial drug distribution is

unif
effe
exis
osm
with
fron
othe
mea

W
by I

$\frac{\partial c}{\partial t} =$

with

$c(x$

and

$\left. \frac{\partial c}{\partial x} \right|$

*Thi
disru
Rele
rpm
and
hour
take
ferer
lack
**Tl

mate
the
relea
***Q

effec
strer

†The
verif

are c
††In

of t
pore

the
is in

allow
refer
††W

for

time

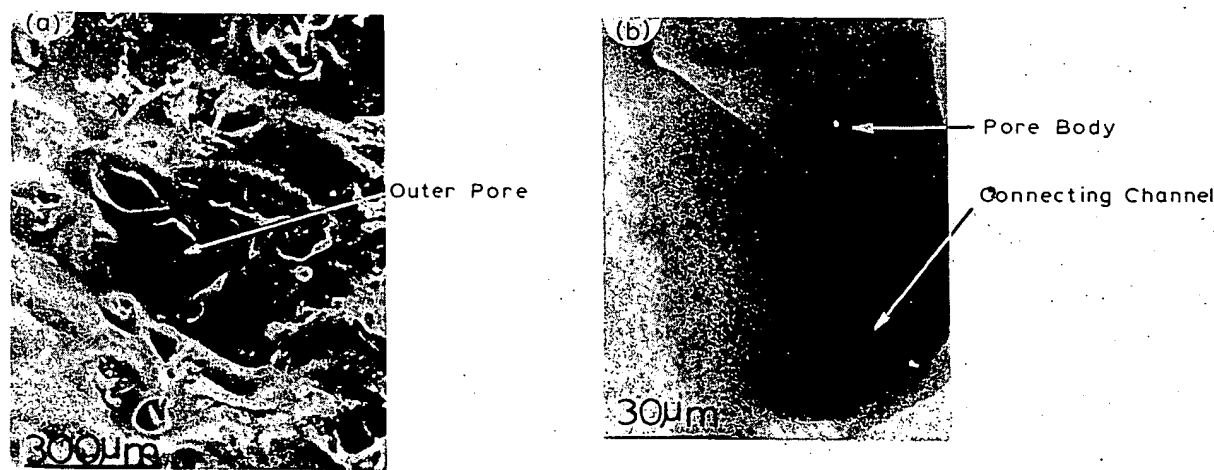


Fig. 2. Scanning electron micrographs (SEM) of controlled release polymers.

(a) Surface of drug-containing EVAc matrix after termination of release (60 h). The average pore size is $101 \pm 33 \mu\text{m}$, in the same size range as the pores and particles in Figs. 1b–d. Controls consisting of pure EVAc matrices and EVAc matrices containing drugs before release show no such pore structure [25]. Loading = 0.25, particle size = 63–149 μm .

(b) 10 \times magnification of one of the outer pores in (a). Notice that there is a channel leading to an inner pore at the base of the outer pore. The pore body is the inside of the outer pore.

uniform (Figs. 1,6). (6) No boundary layer effects exist*. (7) Infinite sink conditions exist**. (8) Minimal effects exist due to osmosis or charge interaction of the drug with the polymer***. (9) Release occurs from only one face of the slab, since the other five faces are coated with an impermeable wax†.

With these assumptions, release is modeled by Fick's second law [20]:

$$\frac{\partial c}{\partial t} = D_e \frac{\partial^2 c}{\partial x^2}, \quad 0 < x < L \quad (1)$$

with the boundary conditions

$$c(x = L, t) = 0 \quad (2)$$

and

$$\left. \frac{\partial c}{\partial x} \right|_{x=0} = 0 \quad (3)$$

*This was verified by stirring, which would have disrupted boundary layers had they been present. Release rates of slabs stirred in containers at 2000 rpm were compared to those that were on the shaker and those that were not shaken at all. Over a 400-hour time period (through 60% release; data were taken at 17 different timepoints) there was no difference in any of the release rates. This indicates the lack of boundary layer effects.

**The volume of the release medium was approximately 100 times the volume of the slab. Increasing the release medium volume does not alter measured release kinetics.

***Consonant with this assumption, we found no effect on release rate due to increasing the ionic strength of the medium from 0 to 1 M NaCl [11].

†The impermeability of the paraffin wax has been verified by control experiments where all faces are coated with wax.

††In this paper concentrations are expressed in terms of the whole matrix including both the aqueous pore space and the polymer. This is in contrast to the more common usage, in which concentration is in terms of the aqueous pore space alone. This allows us to write Fick's second law (eqn. 1) without reference to the matrix porosity.

†††We have chosen cm²/h instead of cm²/s as the unit for the diffusion coefficients because it reflects the time scales over which observations were made.

(corresponding to the situation where drug flow into the release medium occurs at $x = L$), and the initial condition

$$c(x, t = 0) = C_0, \quad 0 < x < L \quad (4)$$

In eqns. (1)–(4), L is the thickness (cm) of the slab, t is time (h), x is a position within the slab (cm), $c(x, t)$ is the local drug concentration (mg/cm³ slab)^{††}, and C_0 is the initial drug concentration. D_e is the effective diffusion coefficient (cm²/h)^{†††}, which is defined and discussed below.

The solution to eqns. (1)–(4) is [20]

$$c(x, t) = \frac{4C_0}{\pi} \sum_{n=0}^{\infty} \frac{(-1)^n}{2n+1} \times \exp[-(2n+1)^2 \pi^2 D_e t / 4L^2] \cos \frac{(2n+1)\pi x}{2L} \quad (5)$$

The cumulative fraction of drug released (i.e., the amount released divided by the amount originally incorporated), is given by [20]

$$\frac{M_t}{M_{\infty}} = 1 - \frac{8}{\pi^2} \sum_{n=0}^{\infty} \frac{1}{(2n+1)^2} \times \exp[-(2n+1)^2 \pi^2 D_e t / 4L^2] \quad (6)$$

Figure 3 contains fits of eqn. (6) to release kinetic curves for BSA released from EVAc slabs, with various drug loadings and particle sizes. The effective diffusivity, D_e , is a free parameter whose value for each loading and particle size is determined by the fit to the corresponding kinetic curve.

We assume that D_e is composed of two factors. The first factor is D_0 , the bulk diffusivity of the drug molecule. The second factor, which we shall call F , accounts for geometric effects of the pore structure, which include tortuosity, dead-end pores, and constrictions between pores.

Thus

$$D_e = D_0 F \quad (7)$$

Since D_0 is either measureable or obtainable from the literature, the pore structure dependent factor F can be extracted from the fits in Fig. 3.

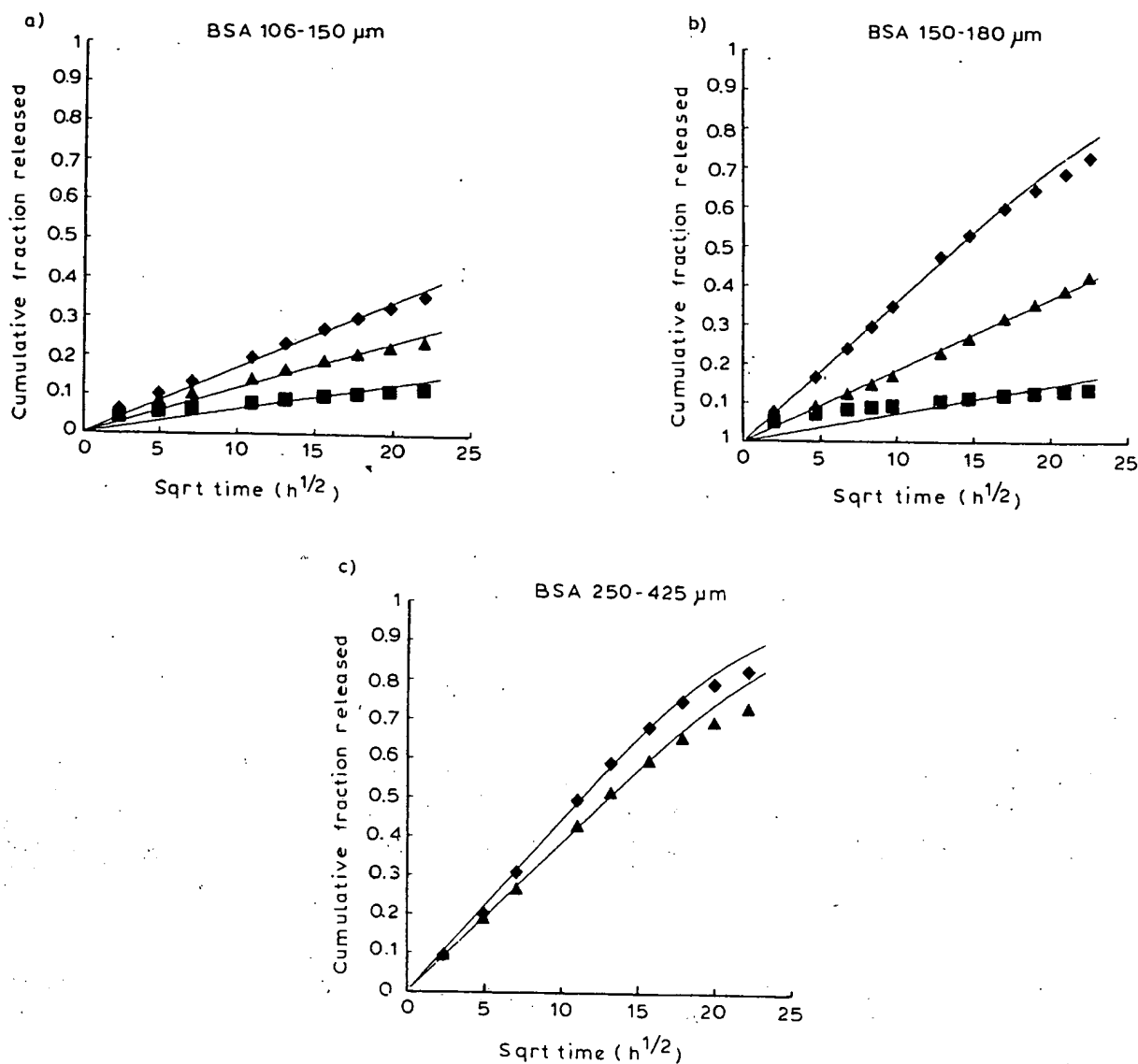


Fig. 3. Experimental release kinetics for matrices containing BSA, where BSA powder particles sizes and loadings are varied. Each point represents the mean of 8 values.

(a) Particle size 106–150 μm . Standard deviations at all points are < 0.08 : \blacksquare — loading = 0.20, porosity (ϵ) = 0.16; \blacktriangle — loading = 0.25, $\epsilon = 0.21$; \blacklozenge — loading = 0.30, $\epsilon = 0.26$.

(b) Particle size 150–180 μm . Standard deviations at all points are < 0.15 : \blacksquare — loading = 0.20, $\epsilon = 0.16$; \blacktriangle — loading = 0.25, $\epsilon = 0.21$; \blacklozenge — loading = 0.30, $\epsilon = 0.25$.

(c) Particle size 250–425 μm . Standard deviations at all points are < 0.20 : \blacktriangle — loading = 0.25, $\epsilon = 0.27$; \blacklozenge — loading = 0.30, $\epsilon = 0.33$.

A log–log plot of F versus porosity (see Fig. 4) was well fit by the function

$$\log_{10} F = 0.463 + 5.64 \log_{10} \epsilon \quad (8)$$

where ϵ is the porosity. Knowing this equation for F , and using eqn. (7), we can then write

$$D_e = D_0(2.904\epsilon^{5.64}) \quad (9)$$

and this value of D_e can be substituted into eqn. (6) to predict release kinetics for slabs with other porosities.

A test of our model is to cast slabs using other proteins, measure the parameters L ,

ϵ , and
follo
This

$F(\epsilon)$

0.

0.0

Fig.
tion
are s
cm²/
each
dete:
Line

Fig.
dat:
(a)
Sta
loa
(b)
dar

ϵ , and D_0 , and see whether the release kinetics follow eqn. (6) with D_e given by eqn. (9). This has been done for β -lactoglobulin and

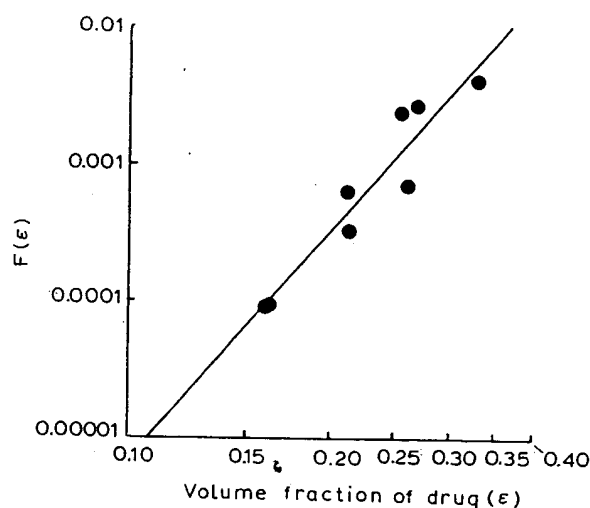


Fig. 4. Log-log plot of factor $F = D_e/D_0$ as a function of porosity for BSA matrices whose kinetics are shown in Fig. 3a-c. D_0 for BSA is 2.52×10^{-3} cm²/h [18] (value corrected for $T = 25^\circ\text{C}$). For each combination of loading and particle size, D_e was determined using the best fit of eqn. (6) to the data. Line is best fit of data, and determines eqn. (8).

lysozyme (Fig. 5). The solid lines are predictions based on eqns. (6) and (9), which show general agreement with the data. The differences that are observed between prediction and experiment may be due to contributions due to differences in the shapes of the protein powders incorporated into the device (which could affect pore geometry), or to deviations from assumptions 1-8 for the cases studied.

An additional test of the model is to determine whether it can predict the time-dependent concentration profile of the drug within the matrix. Concentration profiles of a BSA slab with loadings, measured at four timepoints, are shown in Fig. 6. The curves in Fig. 6 are the predictions of eqn. (5), with D_e determined by fitting eqn. (6) to the accompanying release kinetic data. The fits are quite good, considering the difficulties in the experimental techniques used to obtain the concentration profile.

The above equations have several limitations. It is not expected that they will apply (a) at low loadings (<15%), where the pore space may not be interconnected [21],

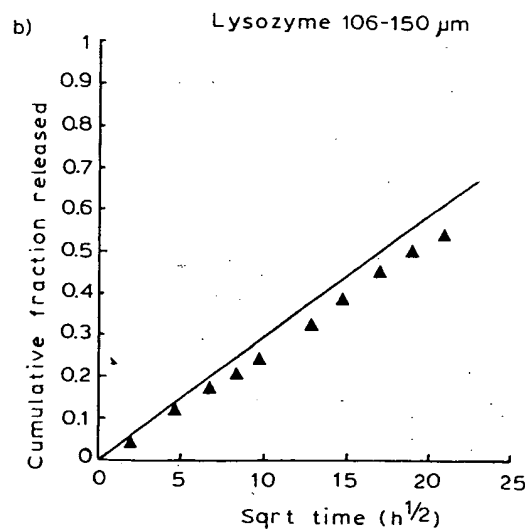
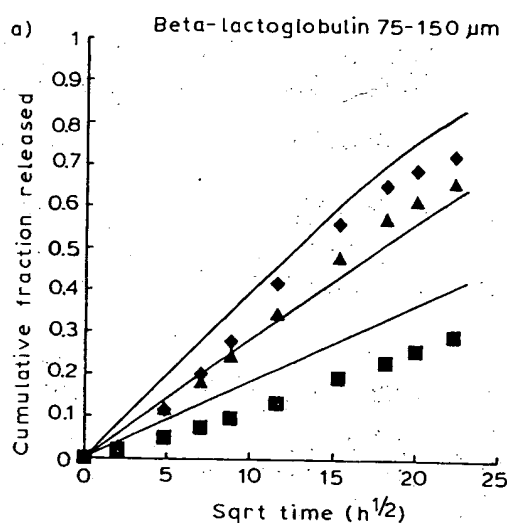


Fig. 5. Release kinetics of β -lactoglobulin and lysozyme. Lines are predictions based on eqns. (6) and (9). Each data point represents the mean of 8 values.

(a) β -lactoglobulin: particle size = 75-150 μm , $D_0 = 2.82 \times 10^{-3}$ cm²/h [26] (value corrected for $T = 25^\circ\text{C}$). Standard deviations at all points are <0.04: \blacksquare — loading = 0.25, $\epsilon = 0.21$; \blacktriangle — loading = 0.40, $\epsilon = 0.27$; \blacklozenge — loading = 0.50, $\epsilon = 0.32$.

(b) Lysozyme: particle size = 106-150 μm , $D_0 = 3.74 \times 10^{-3}$ cm²/h [27] (value corrected for $T = 25^\circ\text{C}$). Standard deviations at all points are <0.04: \blacktriangle — loading = 0.40, $\epsilon = 0.27$.

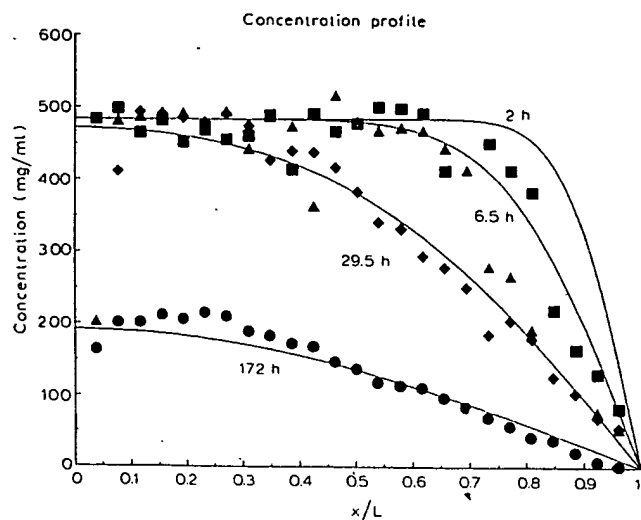


Fig. 6. Drug distribution inside the matrix as a function of time and normalized (x/L) position. Slabs containing BSA at loading 0.5 were released into 100 ml volumes of 0.9% NaCl for varying periods of time. A cryomicrotome (Damon/IEC) was used to serially section the partially released polymer matrices. Protein concentration was determined by UV spectroscopy. Data are indicated by symbols. Each symbol represents the mean concentration of 4 samples. Lines are predictions of eqn. (5). D_e was determined directly by fitting eqn. (6) to the release data. C_0 was directly determined to be 484 mg/(cm³ matrix) using weight of protein fraction and volume of matrix. ■ — 2 hours; ▲ — 6.5 hours; ♦ — 29.5 hours; ● — 172 hours.

or (b) for macromolecules whose solubility is less than 250 mg/ml, where the assumption of rapid drug dissolution may be incorrect. In the latter case, moving-zone models may be more applicable [22].

It should also be recognized that the relation between the F factor and the porosity (eqn. 9) is empirical, and may not be useful outside its known range of validity ($0.15 \leq \epsilon \leq 0.35$).

The diffusion equations used in the current study are simplifications of more complex processes. The factor F must take into account those matrix pore geometric factors contributing to decreases in diffusion rates. Such factors may include pore "tortuosity", dead-end pores, and constrictions between pores [21]. The understanding of such

factors will be important in further developing macromolecular delivery systems.

Although the present study reports *in vitro* release data, we have previously shown that *in vitro* and *in vivo* release rates of macromolecules from identical EVAc slabs are identical [23]. While the release rates from the slabs decrease with time, constant release is attainable from EVAc systems with appropriate geometric design [24].

The present study helps to explain why macromolecules can slowly permeate through normally impermeable polymers. The data should be useful in the design of release vehicles for various polypeptides, polysaccharides, and other bioactive agents now produced by genetic engineering. Such substances often possess very short *in vivo* life times (e.g., growth hormone, interferon) [21], and conventional dosage forms cannot, in general, be used to deliver these drugs. The methodology developed here may be of value in the design of systems for long-term delivery of macromolecules.

ACKNOWLEDGMENTS

This work was supported by NIH grant GM26698. We thank Dean Hsieh and Andrew Braunstein for assistance.

REFERENCES

1. R. Langer and J. Folkman, Polymers for the sustained release of proteins and other macromolecules, *Nature*, 263 (1976) 797–800.
2. R. Langer, H. Fefferman, P.V. Grysky and K. Bergman, A simple method for studying chemotaxis using sustained release of attractants from inert polymers, *Can. J. Microbiol.*, 26 (1980) 274–278.
3. M.L. Hedblom and J. Adler, Genetic and biochemical properties of *Escherichia coli* mutants with defects in serine chemotaxis, *J. Bacteriol.*, 144 (1980) 1048–1060.
4. B.M. Glaser, P.A. D'Amore, R.G. Michels, A. Patz and A. Fenselau, Demonstration of vasoproliferative activity from mammalian retina, *J. Cell Biol.*, 84 (1980) 298–304.

- 5 D. Gospodarowicz, H. Bialecki and T.K. Thakral, The angiogenic activity of the fibroblast and epidermal growth factor, *Exp. Eye Res.*, 28 (1979) 501-514.
- 6 R. Langer and J. Murray, Angiogenesis inhibitors and their delivery systems, *Appl. Biochem. Biotechnol.*, 8 (1983) 9-24.
- 7 M.E. Plishkin, S.M. Ginsberg and N. Carp, Induction of neovascularization by mitogen-activated spleen cells and their supernatants, *Transplantation*, 29 (1980) 255-258.
- 8 M. Mayberg, R.S. Langer, N.T. Zervas and M.A. Moskowitz, Perivascular meningeal projections from cat trigeminal ganglia: Possible pathway for vascular headaches in man, *Science*, 213 (1981) 228-230.
- 9 M. Moskowitz, M. Mayberg and R. Langer, Controlled release of horseradish peroxidase from polymers; A method to improve histochemical localization and sensitivity, *Brain Res.*, 212 (1981) 460-465.
- 10 H.M. Creque, R. Langer and J. Folkman, One month sustained release of insulin from a polymer implant, *Diabetes*, 29 (1980) 37-41.
- 11 R. Langer, D.S.T. Hsieh, L. Brown and W. Rhine, Polymers for the sustained release of macromolecules: Controlled and magnetically modulated systems, in: A.G. Bearn (Ed.), *Better Therapy with Existing Drugs*, Biomedical Information Corporation, New York, 1980, pp. 179-210.
- 12 I. Preis and R. Langer, A single step immunization by sustained antigen release, *J. Immunol. Meth.*, 28 (1979) 193-197.
- 13 W.D. Rhine, D.S.T. Hsieh and R. Langer, Kinetics of polymeric delivery systems for proteins and other macromolecules, *J. Pharm. Sci.*, 69 (1980) 265-270.
- 14 R. Langer, Polymers for sustained release of macromolecules: Their use in a single-step method of immunization, *Meth. Enzymol.*, 73 (1981) 57-75.
- 15 S.J. Desai, P. Singh, A.P. Simonelli and W.I. Higuchi, Investigation of factors influencing release of solid drug dispersed in inert matrices. II: Quantitation of procedures, *J. Pharm. Sci.*, 55 (1965) 1224-1229.
- 16 E.S. Miller, N.A. Peppas and D.N. Winslow, Morphological changes of ethylene/vinyl acetate based controlled delivery systems during release of water-soluble solutes, *J. Membrane Sci.*, 14 (1983) 79-92.
- 17 T.J. Roseman and W.I. Higuchi, Release of medroxyprogesterone acetate from a silicone polymer, *J. Pharm. Sci.*, 59 (1970) 353-357.
- 18 A.A. Kozinski and E.N. Lightfoot, Protein ultrafiltration: A general example of boundary layer filtration, *AIChE J.*, 18 (1972) 1030-1040.
- 19 R.A. Siegel and R. Langer, Computer models of factors causing slow release of macromolecules from hydrophobic polymer matrices, in: *Proc. 11th International Conference of the Controlled Release of Bioactive Agents*, 1984, pp. 92-93.
- 20 J. Crank, *Mathematics of Diffusion*, Clarendon Press, Oxford, 1975.
- 21 R.A. Siegel and R. Langer, Controlled release of polypeptides and other macromolecules, *Pharm. Res.*, 1 (1984) 2-10.
- 22 T. Higuchi, Rate of release of medicaments from ointment bases containing drugs in suspension, *J. Pharm. Sci.*, 50 (1961) 874-875.
- 23 L.R. Brown, C.L. Wei and R. Langer, *In vitro* and *in vivo* release of macromolecules from polymeric drug delivery systems, *J. Pharm. Sci.*, 72 (1983) 1181-1185.
- 24 D.S.T. Hsieh, W. Rhine and R. Langer, Zero order controlled release polymer matrices for micromolecules and macromolecules, *J. Pharm. Sci.*, 72 (1983) 17-22.
- 25 R.S. Bawa, Controlled release of macromolecules from ethylene-vinyl acetate copolymer matrices: Microstructure and kinetic analyses, Master's Thesis, MIT, 1981.
- 26 A.L. Lehninger, *Biochemistry*, Worth Publishers, New York, 1977, p. 176.
- 27 J.T. Edsall, The size, shape, and hydration of protein molecules, in: H. Neurath and K. Bailey (Eds.), *The Proteins*, Vol. 1, Academic Press, New York, 1953, pp. 549-726.